Simulation Modelling Practice and Theory 86 (2018) 155–168

Contents lists available at ScienceDirect

Simulation Modelling Practice and Theory

journal homepage: www.elsevier.com/locate/simpat

Two-phase simulation-based location-allocation optimization of biomass storage distribution

Sojung Kim[a,*], Sumin Kim[b], James R. Kiniry[c]

[a] Department of Engineering and Technology, Texas A&M University–Commerce, 2200 Campbell St, Commerce, TX 75429-3011, USA
[b] Oak Ridge Institute for Science and Education, Oak Ridge, TN 37831, USA
[c] Grassland, Soil and Water Research Laboratory, U.S. Department of Agriculture-Agricultural Research Service (USDA-ARS), Temple, TX 76502, USA

ARTICLE INFO

Keywords:
Agent-based modeling
ALMANAC
Location-allocation
Network partitioning
Biomass storage
Renewable energy

ABSTRACT

This study presents a two-phase simulation-based framework for finding the optimal locations of biomass storage facilities that is a very critical link on the biomass supply chain, which can help to solve biorefinery concerns (e.g. steady supply, uniform feedstock properties, stable feedstock costs, and low transportation cost). The proposed framework consists of two simulation phases: (1) crop yield estimation using a process-based model such as Agricultural Land Management Alternative with Numerical Assessment Criteria (ALMANAC) and (2) biomass transportation cost estimation using agent-based simulation (ABS) such as AnyLogic® with geographic information system (GIS). The OptQuest® in AnyLogic is used as an optimization engine to find the best locations of biomass storage facilities based on evaluation results given by the two-phase simulation framework. In addition, network partitioning and integer linear programming techniques are used to mitigate computation demand of the optimization problem. Since the proposed hybrid simulation approach utilizes realistic biofuel feedstock production and considers dynamics of supply chain activities, it is able to provide reliable locations of biomass storage facilities for operational excellence of a biomass supply chain.

1. Introduction

Given the increasing concerns of future energy security and sustainability, renewable energy has gained attention in both academia and industry. Unlike other renewable energy sources, biomass is a fully renewable resource that can directly produce energy through combustion [47], or indirectly produce energy through conversion of it to various forms of biofuel [4]. Biomass resources are made from biological materials such as grasses, trees, and municipal solids [7]. Among biomass resources, the majority of currently produced renewable fuels are ethanol produced from first-generation biomass feedstocks including corn (*Zea mays* L.) and sugarcane (*Saccharum officinarum*) [42]. However, this widespread use of food crops has negative impacts on the agricultural commodity market. Corn prices go up with increased ethanol production [35]. This negative effect of first generation biomass feedstock on food prices is moving research into the use of cellulosic biomass resources for biofuel production [8]. Cellulosic biomass resources, also known as second generation biomass feedstocks, include dedicated energy crops cultivated primarily for biofuel production [3]. Among dedicated energy crops, switchgrass (*Panicum virgatum*) has been recommended as a key potential cellulosic feedstock for low input bioenergy production in U.S. [10,33,50].

Switchgrass is a tall C_4 perennial, warm-season grass that grows quickly and produces high yield [20]. Moreover, this species has

* Corresponding author.
E-mail addresses: sojung.kim@tamuc.edu (S. Kim), sumin.kim@ars.usda.gov (S. Kim), jim.kiniry@ars.usda.gov (J.R. Kiniry).

https://doi.org/10.1016/j.simpat.2018.05.006
Received 16 January 2018; Received in revised form 3 April 2018; Accepted 8 May 2018
Available online 09 May 2018
1569-190X/ Published by Elsevier B.V.

high tolerances to various environmental stresses, making it capable of maintaining high productivity in marginal locations not suited for food crop production [41]. Switchgrass has been studied extensively for biofuel production [36,51]. Numerous scientific studies have investigated factors that affect yields of switchgrass [11,24,31]. These factors include fertilizer inputs, geographic adaptation, stand age, cultivars and harvest frequency. Unlike the first-generation feedstocks (e.g. corn and sugarcane), cellulosic biofuel has not been fully utilized at a commercial scale due to high feedstock cost resulting from the uncertainty of biomass production [12,15,18]. The reliance of biorefineries on local areas of feedstock production is affected by year to year variability in local climate conditions [44,45]. Moreover, transportation costs for supplying sufficient amounts of biomass feedstock to a biorefinery facility are still high, which is a major obstacle to creating an economically sustainable biofuel production system [9,52]. Development of a sustainable commercial-scale biofuel production system involves not only efficient production of biofuel feedstock but also a biofuel feedstock supply planning and management system that minimizes operational costs of a biofuel supply chain while optimizing biofuel feedstock production under various climatic and environmental conditions [6,9].

Efficient sustainable biofuel supply chain planning and management requires the analyses of economic impacts of expanded biofuel production. The goal of this study is to propose a hybrid simulation-based location-allocation approach addressing opportunities to develop technologies that enhance economical sustainability of biofuel feedstock production, supply chains, and the operation of storage facilities and biorefineries using a holistic analysis framework. The proposed approach adopts two high fidelity simulation paradigms: (1) a process-based model, Agricultural Land Management Alternatives with Numerical Assessment Criteria (ALMANAC) and (2) agent-based simulation (ABS), AnyLogic®. The ALMANAC model was shown to reasonably simulate switchgrass productivity at diverse sites in U.S. [24,29]. In this study, ALMANAC simulates switchgrass productivities at multiple sites in Southern Great Plains of U.S. The AnyLogic model captures detail activities (e.g., loading, unloading, and storing feedstocks) among the actors (e.g. farms, storage facilities, and biorefineries) in the biomass supply chain. Further, OptQuest® which is a search-based meta-heuristic optimization engine available in AnyLogic will find appropriate locations for storage facilities based on results of two simulation models. To mitigate computational demand of the proposed simulation-based optimization approach, network partitioning and linear integer programing are devised (see Section 3 for more detail).

The organization of the paper as follows: Section 2 will briefly introduce existing studies associated with location-allocation approaches for biofuel supply chain management. A two-phase simulation-based framework for location-allocation of biofuel storage facilities will be introduced in Section 3. Section 4 will demonstrate the proposed approach with real data in Southern Great Plains, U.S. Section 5 will discuss conclusion and future work associated with this study.

2. Location-allocation of biomass storage facilities

A biomass supply chain for biofuel is mainly comprised of the biomass suppliers, the storage facilities, and the biorefinery facilities, and the transportation. Fig. 1 represents a generic supply chain model.

Delivered feedstocks are converted into finished goods (e.g., bioethanol, corn oil and distiller's dry grains) at a biorefinery, and the finished product is transported via trucks to terminals for blending. Blending the ethanol with gasoline is carried out so that the ethanol product will be used for fuel purposes only. This is usually done at the initial stage by denaturing it with other chemicals. The blending of ethanol and gasoline ensures the provision of various grades of ethanol and gasoline combinations such as E85 and E15. The E85 consists of 85% ethanol and 15% of gasoline, while the E15 consists 15% of ethanol and 85% of gasoline. The blended ethanol is subsequently sent to the gasoline retail outlets, where they are sold together with other types of fuel [34].

In most cases, the feedstock or raw materials are transported from farms directly to the biorefinery. However, storage facilities between are sometimes needed between farms and biorefineries to ensure raw material freshness and increase the conversion rate [2]. Particularly, because each crop has its own seasonal nature (i.e., a cultivation period) based on environmental conditions,

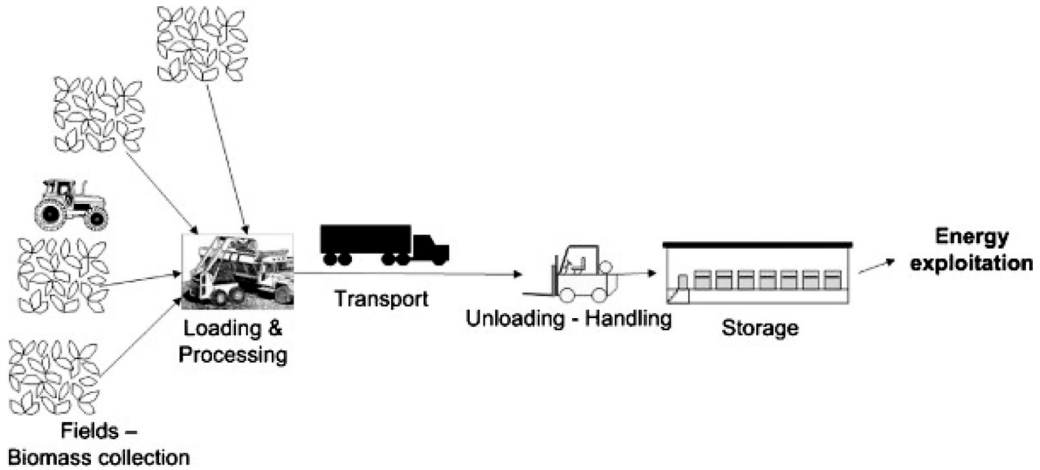

Fig. 1. Generic biomass supply chain design. (Source from Rentizelas et al. [55]).

handling annual variability of biomass supply is a critical challenge in biofuel supply chain management. For instance, the corn in the U.S. Corn Belts mainly harvested from September through November [37]. However, the demand for transportation fuels is year-round. Therefore, there is necessity to manage the biomass storage in order to maintain a continuous supply for production at biorefineries [52].

There are several approaches to minimize operational cost of a biomass supply chain. The most popular approach is transportation scheduling with numerical algorithms and closed-form equations such as non-linear programming and mixed-integer programming [19]. Chen and Fan [6] introduced bioethanol supply chain system planning model based on a mixed integer programing (MIP) to allocate feedstock resources and minimize operational cost. Ekşioğlu et al. [14] proposed a mixed-integer programming model to allocate locations of biorefineries which minimizes the total operational cost involving harvesting, storing, transporting and processing biomass. Lim and Ouyang [34] proposed a design method of a biofuel supply chain network via mixed-integer linear program (MILP). Theoretically, these methods find a way to mitigate operational cost of the biofuel supply chain. However, the closed-form equations are not able to consider complex activities (e.g., shipping and storing feedstocks) in a supply chain and environmental dynamics (e.g., climate change) so that generated schedules may not be feasible in practice.

To overcome the limitation of numerical algorithms, Zhang et al. [53] proposed the geographic information system (GIS)-based approach to select biofuel facilities' locations. In this approach, all detail data such as candidate locations, potential harvesting areas, and transportation distances are given by a GIS data set such as the Michigan Geographic Data Library. Similar to existing approaches using numerical algorithms and closed-form equations, this approach uses a mixed integer linear program (MILP) to find location of biorefineries for transportation cost minimization of a biofuel supply chain. However, since the approach uses detailed GIS information (e.g., country boundaries, a railroad transportation network, a state/federal road transportation network, water body dispersion, city and village dispersion, a population census, biomass production, and location of co-fired power plants), it is suitable to identify realistic locations of facilities. The selected locations can be used as inputs for supply chain simulation so that a user can conduct what-if analysis considering costs and flows under the pre-defined supply chain network.

Although this approach has many benefits, it does not consider environmental dynamics affecting potential yields of feedstocks. The significant influence of environmental factors (e.g. temperature, precipitation, etc.) on switchgrass yield has been well documented by numerous scientific studies. Kandel et al. [21] have reported that high temperature increases rates of stem elongation and leaf elongation, which leads to increased 'Alamo' switchgrass yield. Precipitation also has significant positive effects on switchgrass yield [48]. Besides environmental factors, crop management (e.g. fertilizer input) plays an important role in plant growth and development. The nitrogen (N) fertilizer rate is a significant factor that influences switchgrass yield [10]. Higher yields of switchgrass have been achieved with greater N fertilizer application rates [16]. Given the strong interaction between switchgrass biomass and weather and management, it is important to predict environmental and management variations in yield for switchgrass. This will provide reliable yield estimates for biorefineries and reduce producers' risk. The ALMANAC model is a useful field-scale agricultural simulation tool for quantifying plant yields in diverse conditions because this model simulates plant growth and development simultaneously and realistically, using daily time step inputs for weather (e.g. precipitation, solar radiation, temperature, etc.) and cropping management strategies (e.g. irrigation, fertilizer, planting, etc.). Moreover, ALMANAC successfully predicts switchgrass growth and biomass at diverse locations across the southern U.S. [24,28]. Because the approach proposed by Zhang et al. [53] does not consider environmental dynamics affecting potential yields of feedstocks, it cannot consider a biofuel supply chain with a new cellulosic biofuel feedstock such as "Alamo" switchgrass. In other words, the approach only uses historical production data of existing feedstocks (e.g., corn and sugarcane) so that it is no longer useful when the historical yield is not available and when we consider new feedstocks. Thus, the challenge remains to estimate potential feedstock production regarding environmental dynamics affecting plant growth. The limitations lead to generate an undependable location-allocation framework of storage facilities in a biofuel supply chain under hypothetical conditions.

3. Two-phase simulation-based location-allocation of biomass storage facilities

The proposed approach has distinct inputs and outputs (Fig. 2). As mentioned in Introduction, this study aims at introducing a two-phase simulation-based location allocation approach for biomass storage facilities to minimize the total operational cost of the biofuel supply chain. The proposed approach consists of two major modules: ((1) ALMANAC-based plant yield estimation module and (2) agent-based location-allocation of potential storage facilities. The former is used to estimate potential switchgrass yields under different soil and climate environmental conditions. Section 3.1 addresses the estimation procedure via ALMANAC in great detail. Once potential plant yields are estimated, the information is used as an input in the agent-based location-allocation module. In addition, major characteristics (e.g., a supply chain topology and seasonal demand, operational schedule, and capacity of biorefineries) of biomass supply chain are incorporated in the location-allocation module. Under the given input, the location-allocation module finds the best candidate storage sites over multiple iterations. The optimization problem is solved via OptQuest®, which uses a meta-heuristic algorithm to find the near optimal solution under the inputs given by AnyLogic. Although the meta-heuristic algorithm is not guaranteed to find the exact optimal solution, it efficiently achieves a near optimal solution. Regarding complexity of a biofuel supply chain network, the practicality is a significant aspect in the design of a new approach. Moreover, we believe that a reliable solution can be generated by considering a relatively accurate search space given by a highly detailed simulation model. Detail procedure of the location-allocation is addressed in Section 3.3. As a result, the proposed approach ends when the best candidate storage sites are found in terms of operational cost of the biomass supply chain.

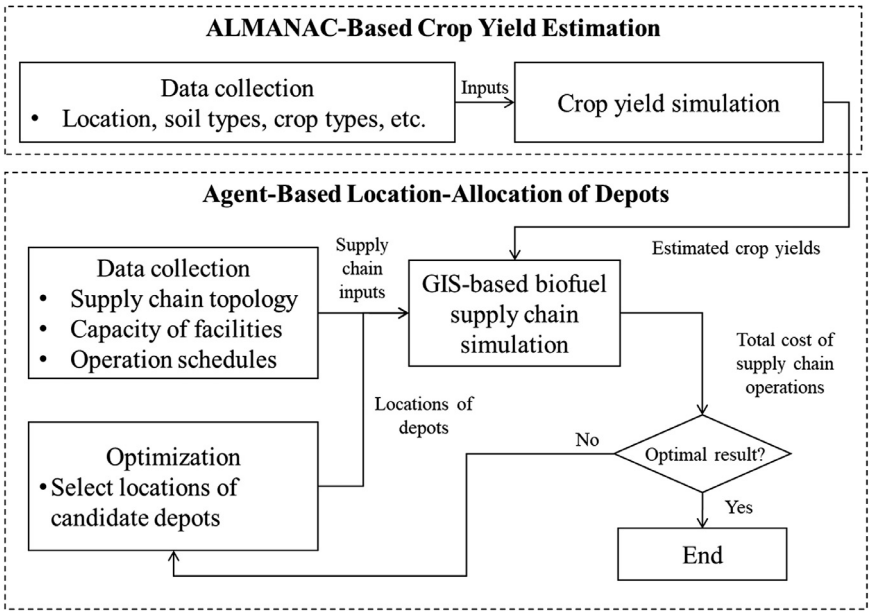

Fig. 2. Proposed two-phase simulation-based location-allocation framework.

3.1. ALMANAC-based plant yield estimation

"Alamo" switchgrass yield data were obtained from peer-reviewed journal articles and summarized in Table 1. The studies were conducted in different years and locations in Southern Great Plains of U.S.

The field data was used to validate the estimation accuracy of the model. Switchgrass yield was simulated by ALMANAC model. Weather data used for each location were from the nearest National Oceanic and Atmospheric Administration [39] station (2017). And for all simulated sites, soil data were obtained from Natural Resources Conservation Service [40]. ALMANAC contains the plant parameters for "Alamo" switchgrass in its plant database that have been validated in the previous studies ([22,27,28,30], and [31] and [23]). The ALMANAC estimates daily plant growth with Leaf Area Index (LAI), light interception, and a constant for converting intercepted light into biomass (radiation use efficiency, RUE) [26]. The value for maximum leaf index (DMLA) was 12 at high planting density of a full season switchgrass, with reduced early-maturity switchgrass and lower planting density. The value for light extinction coefficient for Beer's Law (EXTINC) was 0.33. In the simulation, plant management in the first simulated year consists of fertilizer application, planting, and harvesting. Every year to follow had fertilizer application and harvesting until the final year of harvesting in field trial. The planting date, harvesting date, fertilizer application, and seedling rate varied by locations (see Table 1).

The measured and simulated yields were statistically compared using t-test at $\alpha = 0.05$ (see Fig. 3). The t-test was used to test significant difference between measured and simulated values using Statistical Analysis Software version 9.3 (SAS Institute, NC, USA). The simulated yield averaged over the 2011–2016 period was estimated at each location and was used to incorporate into the biomass supply chain model via ABS.

3.2. Biomass supply chain modeling via agent-based simulation

Similar to the approach proposed by Zhang et al. [53], the proposed approach uses GIS to achieve actual location information of candidate harvesting areas, biomass storage facilities, and biorefineries in a biomass supply chain. However, unlike the previous approach, detailed transportation operations such as ordering, loading and unloading feedstocks between actors are modeled via ABS with GIS in AnyLogic® to achieve realistic transportation cost. In the subject biomass supply chain (Fig. 1), farms deliver raw or preprocessed biomass to either storage facilities or biorefineries, and biomass storages deliver biomass to biorefineries via trucks. We assume that the subject supply chain has the pull system mechanism. In order words, feedstocks are delivered upon requests of other actors.

However, the advantage of the proposed approach is not limited to the GIS. In fact, the major advantage of the proposed approach is its modeling flexibility and capability via ABS which can capture detail activities (e.g., loading, unloading, and storing feedstocks) among the actors (e.g. farms, storage facilities, and biorefineries) in the supply chain. The details of ABS are explained in the following sections.

3.2.1. Biorefinery model

In the simulation, each biorefinery places an order to multiple storage facilities regarding its potential profits and production capacity. Since each biorefinery wants to minimize its operational cost, it tends to purchase feedstock from storage facilities which

Table 1
Summary of switchgrass "Alamo" studies for locations, planting years, harvest years, measured yields, and ALMANAC simulated yield averaged across published harvest years and across years 2011–2016 in different locations in Southern Great Plains of U.S.

Location	Planting year	Harvest year	Measured yield Mg ha^{-1}	Simulated yield	
				Validation Mg ha^{-1}	2011–2016 Mg ha^{-1}
Shorter, AL (32 30′N, 85 40′W)	1989	1990-2009	24[a]	22	23
Fayetteville, AR (36 6′N, 94 10′W)	2008	2009-2010	16[b]	17	13
Gretna, VA (36.93, −79.19)	2008	2009-2015	8.6[c]	11	12
Knoxville, TN (35 57′38″N, 83 55′14″W)	2007	2009-2010	15[d]	14	18
Crossville, TN (35°56′56″ N, 85°56′56″W)	2007	2009-2010	16[d]	15	15
Milan, TN (35°55′11″ N, 88°45′32″ W)	2004	2009-2010	19[d]	20	16
Columbia, MO (38°53′24″ N, 92°12′36″ W)	2009	2011-2015	25[e]	23[i]	26
Mt. Vernon, MO (37°4′48″ N, 93°52′48″ W)	2009	2011-2015	19[e]	17[i]	20
Ardmore, OK (34 10′N, 97 8′W)	2008	2009-2010	16[f]	17	16
Stillwater, OK (36°7′12″ N, 97°5′24″ W)	2009	2011–2015	13[e]	8[i]	11
Calhoun, LA (32°31′12″ N, 92°20′60″ W)	2009	2011, 2012, 2014	27[e]	23[i]	25
Nacogdoches, TX (31°30′0″ N, 94°45′36″ W)	2009	2011-2015	38[e]	23[i]	25
Temple, TX (31°3′0″ N, 97°20′60″ W)	2009	2011-2015	28[e]	18[i]	22

Data obtained from
[a] Bransby and Huang [5];
[b] Ashworth et al. (2016) [1];
[c] Fike et al. [16];
[d] Warwick et al. [49];
[e] Kim et al. [24];
[f] Kering et al. [22].

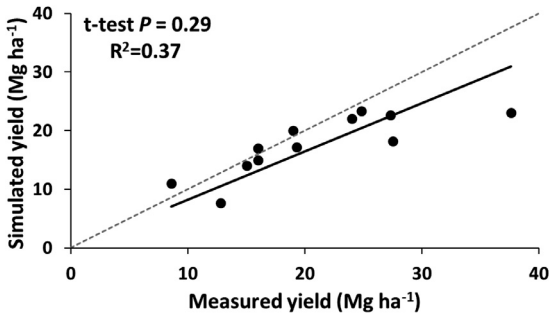

Fig. 3. Measured yields and simulated yields by ALMANAC for switchgrass "Alamo" cultivated in different locations in Southern Great Plains of U.S. The solid line is the regression and the dashed line is the 1:1 line.

mitigates its transportation cost. In this study, an attractiveness concept addressed in the Huff model (1982) is utilized to evaluate preferable storage facilities (i.e., suppliers) of an individual biorefinery [46]. The probability of refinery j from given location traveling to biomass storage k at time t is calculated by Eq. (1).

$$P_{jkt} = C_{kjt}^{S} / \left(\sum_{k \in \mathbf{K}} C_{kjt}^{S} \right) \tag{1}$$

where P_{jkt} is choice probability of refinery j from given location traveling to storage facilities k at time t, and C_{kjt}^{S} is unit transportation cost from storage facilities k to refinery j at time t. K represents a set of candidate sites of storage facilities (see Table 2 for more information). As a result, an individual refinery chooses a storage based on P_{ijt}.

Table 2
Nomenclature.

Sets	
I	A set of biomass farms.
J	A set of biorefineries.
K	A set of candidate sites for storage facilities.
T	A set of planning time horizon.
Constants	
C_{it}^{P}	Unit production cost at farm i at time t for $\forall i \in \mathbf{I}$ and $\forall t \in \mathbf{T}$.
C_{ikt}^{S}	Unit transportation cost from farm i to candidate site k at time t for $\forall i \in \mathbf{I}$, $\forall k \in \mathbf{K}$, and $\forall t \in \mathbf{T}$.
C_{kjt}^{S}	Unit transportation cost from storage k to refinery j at time t for $\forall k \in \mathbf{K}$, $\forall j \in \mathbf{J}$, and $\forall t \in \mathbf{T}$.
C_{ijt}^{S}	Unit transportation cost from farm i to refinery j at time t for $\forall i \in \mathbf{I}$, $\forall j \in \mathbf{J}$, and $\forall t \in \mathbf{T}$.
C_{kt}^{H}	Unit holding cost at candidate site k at time t for $\forall k \in \mathbf{K}$ and $\forall t \in \mathbf{T}$.
P_{jkt}	Probability of refinery j from given location traveling to storage k at time t for $\forall j \in \mathbf{J}$, $\forall k \in \mathbf{K}$, and $\forall t \in \mathbf{T}$.
Q_{jt}^{D}	Demand given by refinery j at time t for $\forall j \in \mathbf{J}$ and $\forall t \in \mathbf{T}$.
Q_{it}^{P}	Production quantity of farm i at time t for $\forall i \in \mathbf{I}$ and $\forall t \in \mathbf{T}$.
Q_{kt}^{H}	Holding quantity at candidate site k at time t for $\forall k \in \mathbf{K}$ and $\forall t \in \mathbf{T}$.
Q_{kt}^{C}	Capacity of candidate site k at time t for $\forall k \in \mathbf{K}$ and $\forall t \in \mathbf{T}$.
Decision variables	
x_k	Binary variable representing presence of a storage at candidate site k; 1: presence; and 0: not presence.
Q_{ikt}^{S}	Transportation quantity from farm i to candidate site k at time t for $\forall i \in \mathbf{I}$, $\forall k \in \mathbf{K}$, and $\forall t \in \mathbf{T}$.
Q_{kjt}^{S}	Transportation quantity from storage k to refinery j at time t for $\forall k \in \mathbf{K}$, $\forall j \in \mathbf{J}$, and $\forall t \in \mathbf{T}$.
Q_{ijt}^{S}	Transportation quantity from farm i to refinery j at time t for $\forall i \in \mathbf{I}$, $\forall j \in \mathbf{J}$, and $\forall t \in \mathbf{T}$.

3.2.2. Biomass farm and storage models

Once a storage receives an order from a biorefinery, it sends stored feedstocks in the facility via a truck. If the storage's stock level reaches its a reorder point, it requests additional feedstocks to a biomass farm selected by Eq. (1). In this study, we assume that an individual biomass farm has its own silo to reduce plant loss. Transportation states can be diagrammed in AnyLogic (Fig. 4).

Initially (Fig. 4a), a truck located at a biomass farm waits for a shipment request sent by a storage. Once it receives the request, it loads feedstocks and delivers them to a storage. Travel time between facilities will be computed based on driving speed (60 miles per h) of a truck and distance given by GIS module in AnyLogic. The truck unloads the feedstocks at a storage and returns to a biomass farm. Similarly, a truck located at a storage delivers feedstocks to a biorefinery upon a request (Fig. 4b). Finally, a truck located at a biomass farm delivers feedstocks to a biorefinery according to a request of a biorefinery (Fig. 4c). The advantage of the proposed model is it accurately estimates transportation costs that are dependent on physical distance between facilities and dynamic ordering process between multiple facilities. In the model, to estimate potential transportation cost under the given historical demand and

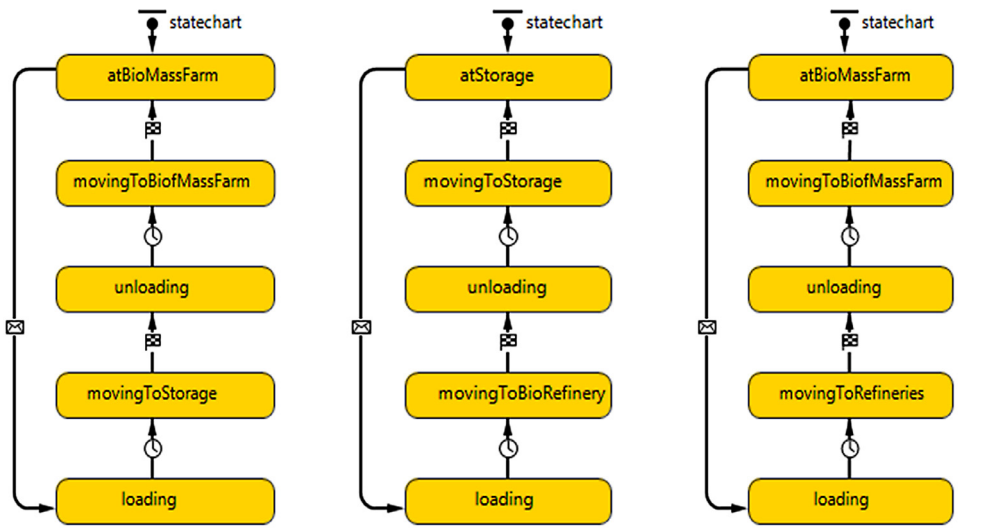

(a) Transportation between a farm and a storage (b) Transportation between a storage and a refinery (c) Transportation between a farm and refinery

Fig. 4. Transportation state diagrams in AnyLogic.

production data, we assume that there are unlimited number of homogeneous trucks with capacity of 20 tonnages.

3.3. Location-allocation integer programming

A goal of mathematical model, i.e. Eq. (2), is to identify locations of storage facilities minimizing operation cost, particularly transportation cost, of an ethanol supply chain.

$$\begin{aligned} Min\ z\ =\ & \sum_{i\in \mathrm{I}}\sum_{t\in \mathrm{T}} C_{it}^{P} Q_{it}^{P} + \sum_{k\in \mathrm{K}} x_k \sum_{i\in \mathrm{I}}\sum_{t\in \mathrm{T}} C_{ikt}^{S} Q_{ikt}^{S} \\ & + \sum_{k\in \mathrm{K}} x_k \sum_{j\in \mathrm{J}}\sum_{t\in \mathrm{T}} C_{kjt}^{S} Q_{kjt}^{S} + \sum_{i\in \mathrm{I}}\sum_{i\in \mathrm{I}}\sum_{t\in \mathrm{T}} C_{ijt}^{S} Q_{ijt}^{S} \\ & + \sum_{k\in \mathrm{K}} x_k \sum_{t\in \mathrm{T}} C_{kt}^{H} Q_{kt}^{H}/2 \end{aligned} \tag{2}$$

In Eq. (2), the first term refers to total production cost of farms; the second term refers to total transportation cost from farms to candidate storage sites; the third term refers to total transportation cost from candidate storage sites to biorefineries; the fourth term refers to total transportation cost from farms to biorefineries; and the last term refers to total holding cost of candidate storage sites. Table 2 shows definitions of sets, constants, and decision variables used in the proposed simulation-based optimization approach.

However, the proposed optimization model, i.e. Eq. (2), requires enormous computation time to find its optimal solution. The number of possible locations of storage facilities is $2^{|\mathbf{K}|}$ and all the cost data (i.e., C_{it}^{P}, C_{ikt}^{S}, C_{kjt}^{S}, C_{ijt}^{S}) are given by ABS so that they will not be a problem to find the solution. On the other hand, there are too many transportation quantity variables (i.e., Q_{ijt}^{S}, Q_{ikt}^{S}, and Q_{kjt}^{S}) need to be explored in the optimizations. For example, if we consider a supply chain network involving 6 candidate storage sites, 13 farms, 24 biorefineries, and monthly time horizon (i.e., 12 months), the numbers of transportation quantity variables becomes 6,408 (see Eq. (3)). Note that C_{kt}^{H} is given by a problem and Q_{kt}^{H} can be achieved based on activities (e.g., supply, demand, and transportation) between actors in the simulation model.

$$\{(|\mathrm{I}| \times |\mathrm{J}|) + (|\mathrm{I}| \times |\mathrm{K}|) + (|\mathrm{K}| \times |\mathrm{J}|)\} \times |\mathrm{T}| = \{(13\ \times\ 24) + (13\ \times\ 6) + (6\ \times\ 24)\} \times\ 12 = 6,408 \tag{3}$$

This implies that the proposed mathematical model cannot be solved via the simulation-based optimization approach in practice due to its computational demand. If the transportation quantities are binary, Eq. (2) has $2^{|6+6408|}$ possible values. Thus, it takes enormous computation time to solve the problem when the proposed approach has to make multiple simulation runs for each alternative (or a parameter set) to consider randomness of input data. Therefore, instead of finding the exact transportation quantities for the optimizations, the proposed approach finds values of the transportation quantities at the beginning of simulation runs under the given value of x_k by OptQuest®. Although this potentially sacrifices solution accuracy of the original optimization, the simulation-based optimization can be practical, particularly, when it deals with a large-scale biomass supply chain. The transportation quantities can be found from Eq. (2) with the following constraints.

$$\sum_{i\in I} Q_{ijt}^{S} + \sum_{k\in K} Q_{kjt}^{S} \le Q_{jt}^{D},\ \text{for}\ \forall\, j \in \mathbf{J}\ \text{and}\ \forall\, t \in \mathbf{T} \tag{4}$$

$$\sum_{k\in \mathrm{K}} Q_{ikt}^{S} + \sum_{j\in \mathrm{J}} Q_{ijt}^{S} = Q_{it}^{P},\ \text{for}\ \forall\, i \in \mathbf{I}\ \text{and}\ \forall\, t \in \mathbf{T} \tag{5}$$

$$Q_{kt}^{H} = \sum_{j\in \mathrm{J}} Q_{kjt}^{S} - \sum_{i\in \mathrm{I}} Q_{ikt}^{S},\ \text{for}\ \forall\, k \in \mathbf{K}\ \text{and}\ \forall\, t \in \mathbf{T} \tag{6}$$

$$Q_{kt}^{H} \le Q_{kt}^{C}\ \text{and}\ Q_{kt}^{H} \ge 0,\ \text{for}\ \forall\, k \in \mathbf{K}\ \text{and}\ \forall\, t \in \mathbf{T} \tag{7}$$

$$Q_{ijt}^{S}\ , Q_{ikt}^{S}, Q_{kjt}^{S} \ge 0,\ \text{for}\ \forall\, i \in \mathbf{I}, \forall\, j \in \mathbf{J}, \forall\, k \in \mathbf{K}\ \text{and}\ \forall\, t \in \mathbf{T} \tag{8}$$

In Eq. (4), the total transportation quantity to refinery j at time t cannot be greater than its demand. In Eq. (5), total supply from farm i to storage facilities and biorefineries equals to its total production quantity. Eqs. (6) and (7) refer to an equation computing holding quantity and its range. Eq. (8) is non-negativity conditions of transportation quantities. This integer linear programing (ILP) problem is solved by Branch and Bound technique [32]. In other words, we initially define values of transportation quantities by solving the ILP model so that the number of decision variables becomes $2^{|\mathbf{K}|}$.

3.4. Network partitioning for simulation run-time reduction

Although this study utilizes ILP to reduce the size of search space, it is still challenging to use the proposed framework due to its evaluation time via ABS, particularly for a large-scale network. According to Kim et al. [24,25], a simulation model with Phoenix, Arizona road network involving about 3 million vehicles requires six hours for a single simulation run. In this case, if we make 30 replications to evaluate each alternative, the optimization will take 480 days to find the solution, which makes it difficult to use the simulation-based optimization approach. From observations about agents' behaviors in the developed ABS, we found that each biorefinery tends to use the closest farms or storage facilities to minimize its transportation costs. This implies that narrowing down the search scope of each refinery will not greatly affect the original results of ABS. Thus, in this section, we are going to extend the

```
1:  CALL G which is a biofuel supply chain network
2:  SET zones involving refineries using K-means clustering
3:  FOR zones in set Z
4:    SORT the farms and storages based on transportation cost from zone z ∈ Z
5:    FOR the sorted list of farms and storages
6:      ADD arc l ∈ L connected to a farm (or a storage) to zone z ∈ Z
7:      IF the total demand of refineries in zone z ∈ Z is less than the total supply of
        connected farms and storages THEN EXIT LOOP
8:    NEXT
9:  NEXT
10: RETURN G and Z
```

Fig. 5. Pseudo code of network partitioning.

network partitioning approach proposed by Kim et al. [24,25] for a biomass supply chain involving three actors (i.e., farms, storage facilities, and biorefineries).

Let $\mathbf{G} = (\mathbf{N}, \mathbf{L}, \mathbf{C^S})$ be the original supply chain network partitioned into $|\mathbf{Z}|$ zones represented as $\mathbf{G}_z = (\mathbf{N}_z, \mathbf{L}_z, \mathbf{C}_z^{\mathbf{S}})$. $\mathbf{N}$ is a set of nodes; $\mathbf{L}$ is a set of arcs; $\mathbf{C^S}$ is a set of transportation cost associated with L; $\mathbf{N_z}$ is a set of nodes in zone z; $\mathbf{L_Z}$ is a set of arcs in zone z; $\mathbf{C}_z^{\mathbf{S}}$ is a set of transportation cost in zone z. The following k-means clustering algorithm [54] will generate initial zones (or partitioned networks)

$$\text{argmin}_{\mathbf{Z}} \left\{ \sum_{z \in Z} \sum_{n \in z} n - \mu_z{}^2 \right\} \tag{9}$$

where μ_z is the mean of nodes in zone $z \in \mathbf{Z}$ and n is a node with two-dimensional coordinate vector in $\mathbf{N}$. Once the $|\mathbf{Z}|$ zones are specified, biomass farms and candidate storage sites close to zone z can be included into the original zone z. Note that a farm (or a candidate site) can be shared by multiple zones to avoid potential supply problems of switchgrass. Fig. 5 reveals pseudo code of the proposed network partitioning algorithm.

As a result, we can have the network G as follows:

$$\mathbf{G} = \bigcup_{z \in \mathbf{Z}} (\mathbf{N}_z, \mathbf{L}_z, \mathbf{C}_z^{\mathbf{S}}) \tag{10}$$

$$\mathbf{N}_z = \{\mathbf{N}_z^{\mathbf{F}} \cup \mathbf{N}_z^{\mathbf{D}} \cup \mathbf{N}_z^{\mathbf{R}}\} \tag{11}$$

where $\mathbf{N}_z^{\mathbf{F}}$ is a node set of farms in zone z, $\mathbf{N}_z^{\mathbf{D}}$ is a node set of candidate storage sites in zone z, $\mathbf{N}_z^{\mathbf{R}}$ is a node set of biorefineries in zone z. This partitioning algorithm reduces not only simulation run-time but also the number of transportation quantity variables as follows:

$$\sum_{z \in \mathbf{Z}} \{(|\mathbf{N}_z^{\mathbf{F}}| \times |\mathbf{N}_z^{\mathbf{R}}| \times |\mathbf{T}|) + (|\mathbf{N}_z^{\mathbf{F}}| \times |\mathbf{N}_z^{\mathbf{W}}| \times |\mathbf{T}|) + (|\mathbf{N}_z^{\mathbf{D}}| \times |\mathbf{N}_z^{\mathbf{R}}| \times |\mathbf{T}|)\} \tag{12}$$

where $\sum_{z \in \mathbf{Z}} |\mathbf{N}_z^{\mathbf{F}}| = |\mathbf{I}|$, $\sum_{z \in \mathbf{Z}} |\mathbf{N}_z^{\mathbf{R}}| = |\mathbf{J}|$, and $\sum_{z \in \mathbf{Z}} |\mathbf{N}_z^{\mathbf{D}}| = |\mathbf{K}|$. If each zone has the same number of nodes, the number of decision variables will become:

$$|\mathbf{Z}||\mathbf{T}| \times \left\{ \left(\frac{|\mathbf{I}| \times |\mathbf{J}|}{|\mathbf{Z}|^2} \right) + \left(\frac{|\mathbf{I}| \times |\mathbf{K}|}{|\mathbf{Z}|^2} \right) + \left(\frac{|\mathbf{K}| \times |\mathbf{J}|}{|\mathbf{Z}|^2} \right) \right\} \tag{13}$$

Thus, the number of transportation quantity variables given by Eq. (3) reduces the number of variables to 224 when there are three partitioned networks including 4 farms, 2 candidate storage sites, and 8 biorefineries each.

4. Experiments

In this study, we consider a biomass supply chain in Southern Great Plains, USA, involving 13 locations of potential switchgrass farms (Table 3). Potential yield is estimated under assumption that existing silage area of corn given by National Agricultural Statistics Service (2015) is used to produce “Alamo” switchgrass. To be more specific, the estimated yield per ha shown in Table 1 is multiplied by the given harvested area to compute total estimated yield at each farm. The estimated production quantities at each farm (Table 3), i.e. Q_{it}^P, under conversion rate of 60 gallons per ton given by Haque and Epplin [17]. For example, in the data set associated with Shorter, AL, the product of 60 gallons per ton and 83,766 ton gives 5 M gallons. The estimated production quantities are used as the potential supply of switchgrass in the ABS model.

In addition, biorefineries in the Southern Great Plains, U.S. are considered assuming that existing biorefineries are able to use “Alamo” switchgrass to produce ethanol. Thus, 24 operating biorefineries in Georgia, Texas, Missouri, Mississippi, Tennessee, and Kansas states are included in the subject supply chain (see Table 4). Since the total operating production quantity (i.e., demand of “Alamo” switchgrass) of subject refineries is much larger than the estimated production quantity of “Alamo” switchgrass shown in Table 3, this study assumes that “Alamo” switchgrass is used to produce only 10% of the total ethanol production of subject refineries.

Table 3
Estimated supply.

Location	Harvested area[a] (ha)	Estimated yield (ton)	Estimated gallons (M gal.)[b]
Shorter, AL	3,642	83,766	5
Fayetteville, AR	809	10,517	1
Gretna, VA	50,586	607,032	36
Knoxville, TN	8,920	160,560	10
Crossville, TN	7,433	111,495	7
Milan, TN	7,929	126,864	8
Columbia, MO	19,824	515,424	31
Mt. Vernon, MO	15,249	304,980	18
Ardmore, OK	5,756	92,096	6
Stillwater, OK	3,957	43,527	3
Calhoun, LA	809	20,225	1
Nacogdoches, TX	48,792	1,219,800	73
Temple, TX	42,937	944,614	57

[a] Harvested area refers to the avg. silage area of Corn given by National Agricultural Statistics Service (2015) [38].
[b] Conversion rate of switchgrass to ethanol is 60 gallons per ton (Haque and Epplin, 2010).

Table 4
Annual production of ethanol biorefineries in 2016 [43] using corn, sorghum (Sorghum *bicolor* (L.) Moench), and wheat (*Triticum aestivum* L.).

Location	Feedstock	Operating production (M gal./year)
Camilla, GA	Corn	120
Garden City, KS	Corn/Sorghum	55
Garden City, KS	Corn/Sorghum	12
Pratt, KS	Corn	55
Phillipsburg, KS	Corn	40
Lyons, KS	Corn	60
Garnett, KS	Corn	42
Liberal, KS	Corn	110
Oakley, KS	Corn	50
Russell, KS	Sorghum/Wheat starch	55
Scandia, KS	Corn	21
Laddonia, MO	Corn	50
St. Joseph, MO	Corn	50
Malta Bend, MO	Corn	50
Macon, MO	Corn	46
Craig, MO	Corn	5
Carrollton, MO	Corn	55
Vicksburg, MO	Corn	54
Obion, TN	Corn	120
Loudon, TN	Corn	105
Levelland, TX	Corn	40
Plainview, TX	Corn	120
Hereford, TX	Corn	110
Hereford, TX	Sorghum/Wheat starch	120

This assumption prevents a case that only one refinery consumes all the switchgrass produced by 13 farms. In addition, average monthly demand and price data of ethanol in U.S., and the monthly demand of each biorefineries Q_{jt}^{D} is estimated based on Tables 4 and 5. The unit transportation cost is assumed to be $1.7 per mile (ATRI, 2016).

Actors in the subject supply chain cover a wide range of locations (Fig. 6). Red, blue, and green circles represent biorefineries, candidate storage sites, and biomass farms, respectively. Six candidate sites (i.e., Dallas, TX, Birmingham, AL, St. Louis, MO, Norman, OK, Wichita, KS, and Jonesboro, AR) of storage facilities are selected regarding the monthly cost of leasing storage space in Southern Great Plains, U.S.

4.1. Simulation model validation

In addition to the validation of the estimated plant yield by ALMANAC with actual measured yield addressed in literatures, this study validates the developed ABS model in terms of travel time because travel time is critical to compute transportation cost of the supply chain. Possible routes between farms and biorefineries varied among 10 examples (Table 6). In this section, we compare the time difference between actual travel and simulated travel.

Avg. travel time, avg. distance, and avg. speed of vehicles in the actual data set of 312 routes are 9.8 h, 638.5 miles, and 65.4 miles/h, respectively. On the other hand, avg. travel time, avg. distance, and avg. speed of vehicles in the simulated data set are

Table 5
Monthly demand and price data of ethanol.

Month	Monthly demand weight[a]	Price[b] ($/gal.)		
		E10	E30	E85
January	0.94	1.92	1.76	1.66
February	0.92	2.01	1.84	1.67
March	1.00	2.18	1.97	1.79
April	0.95	2.30	2.05	1.86
May	1.03	2.51	2.15	1.98
June	1.02	2.61	2.25	2.00
July	1.05	2.43	2.25	1.91
August	1.06	2.46	2.19	1.87
September	1.00	2.29	2.09	1.83
October	1.01	2.27	2.10	1.87
November	1.00	2.10	2.00	1.77
December	1.03	2.09	1.92	1.74

[a] Monthly demand weight is calculated based on consumption fluctuation from 2015 to 2016 [13].
[b] Price refers to avg. price data between 2015 and 2016 [43].

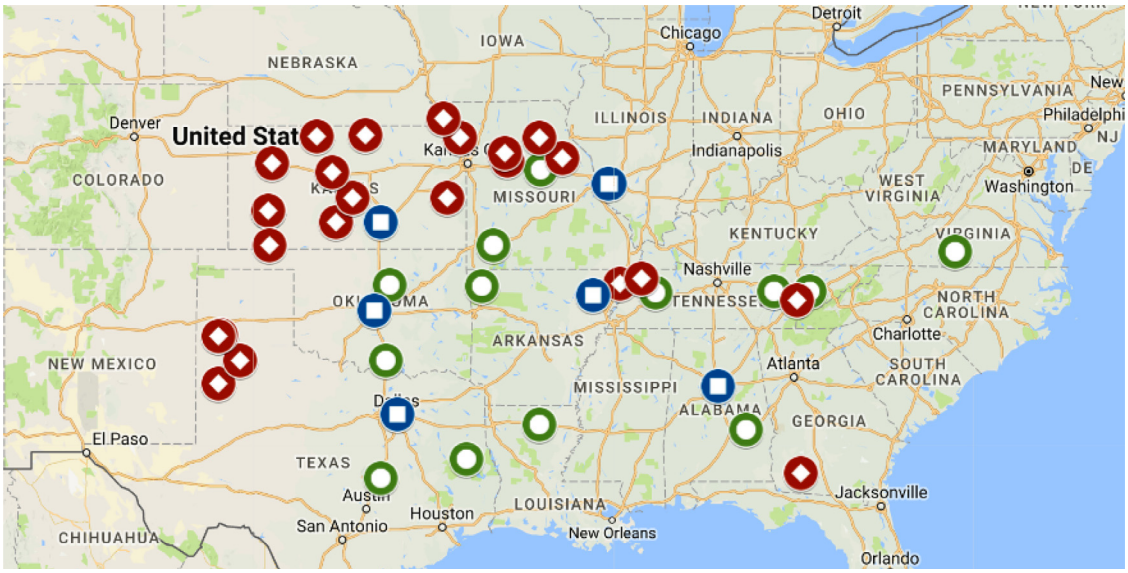

Fig. 6. Google Map® image of the ethanol supply chain in the Southern Great Plains of U.S (red-biorefineries; blue-candidate storage sites; green-biomass farms). (For interpretation of the references to color in this figure legend, the reader is referred to the web version of this article.)

Table 6
Samples of travel time data.

Origin	Destination	Travel time (h)	Simulated travel time (h)	Difference[a]
Plainview, TX	Stillwater, OK	5.82	5.87	−0.05
Craig, MO	Temple, TX	10.63	11.16	−0.53
Craig, MO	Mt. Vernon, MO	4.07	4.16	−0.09
Loudon, TN	Mt. Vernon, MO	10.02	9.72	0.30
Phillipsburg, KS	Mt. Vernon, MO	7.10	6.93	0.17
Laddonia, MO	Mt. Vernon, MO	3.65	3.56	0.09
Pratt, KS	Stillwater, OK	3.28	3.17	0.11
Garnett, KS	Temple, TX	8.78	8.62	0.16

[a] Difference refers to a gap between travel time and simulated travel time.

9.5 h, 638.5 miles, and 65.4 miles/h, respectively. In fact, since we calibrated the ABS model with Geographic Information System (GIS) map, both data sets should have the exactly same avg. distance and avg. speed of vehicles. However, the mean absolute deviation (MAD) between the two travel times is 0.3 h because we do not implement traffic signals and traffic congestions in the ABS

Table 7
Performance of the simulation-based location-allocation.

Category	Number of storage facilities				
	1	2	3	4	5
Travel distance (miles/truck)	776.5	687.5	625.0	613.0	607.7
Travel time (hours/truck)	12.9	11.5	10.4	10.2	10.1
Number of shipments (trucks/day)	188	188	188	188	188
Optimization time (h)	0.7	1.4	1.7	1.2	0.5
Number of iterations	6	15	20	15	6
Total cost ($1,000/day)	115.9	110	107.2	113.4	117.2
Transportation cost ($1,000/day)	109.6	95.7	85.4	83.5	80.4
Holding cost ($1,000/day)	6.3	14.3	21.8	29.9	36.8

model. According to the p-value (0.2182) of the paired t-test between two data sets at $\alpha = 0.05$, there is no significant difference between the two data sets so that we can use the ABS to estimate the transportation cost of a biomass supply chain.

4.2. Performance of the simulation-based location-allocation

The performance of the proposed simulation-based location-allocation approach is evaluated under the different number of storage facilities (Table 7). The first three rows (i.e., travel distance, travel time, and number of shipments) refer to averages associated with transportation in the subject biofuel supply chain. The information is given after we make 30 replications. The daily total cost involving transportation and holding costs is considered as the objective value (see Section 3.3) in this study. The number of iterations represents the iterations to achieve the (near) optimal solution via OptQuest®. Thus, the number of iterations and the optimization time tell us how the optimization engine can quickly find locations of storage facilities. To understand performance of the proposed ILP in Section 3.3, we investigate optimization performance in terms of total cost and search time under different number of storage facilities. In this section, the proposed network partitioning method is not implemented to clearly understand the impact of different numbers of storage facilities on the subject biomass supply chain.

The minimum total cost under the fixed demand of ethanol (i.e., the number of shipments is 188 trucks per day) is achieved when the supply chain has three storage facilities out of six candidate sites between 13 farms and 24 biorefineries. The total cost of the best solution is $107,200 with transportation cost of $85,400. Its optimization time with 600 simulation runs (= 20 iterations × 30 replicates) is 1.7 h so that users can use the proposed simulation-based optimization approach in practice. If the proposed ILP model is not used, 128,160 (= 20 iterations × 6,408 cases) simulation runs needed to find the optimum solution, which will may take 454 days (= 1.7 h × 6,408 cases). Selected candidate storage sites in AnyLogic simulation software are in a wide range of locations (Fig. 7). Storage facilities with red dotted squares represent the selected storage facilities in the optimum solution. The selected storage facilities are in Dallas, TX, Birmingham, AL, and St. Louis, MO.

Average travel time and avg. travel distance decrease as the number of storage facilities increases (Table 7). This is because biorefineries or farms can have a storage near their locations when the supply chain has higher number of storage facilities. Due to trends of avg. travel time and avg. travel distance, transportation costs decrease as the number of storage facilities increase. However, having more storage facilities is not necessarily beneficial to the supply chain due to holding cost. Holding cost increases as the number of storage facilities increases under the assumption that total supply of switchgrass is larger than its total demand. In the simulation model, each storage must have 400 tons of switchgrass as its own safety stock to meet potential delivery requests given by biorefineries so that the holding cost increases according to the number of storage facilities. Therefore, the case with five storage facilities cannot have the minimum total cost even though it has the minimum transportation cost. If we consider different assumptions associated with holding cost, the optimum solution can be changed.

4.3. Performance of network partitioning

The performance of network partitioning in terms of computational demand and solution accuracy varies as the number of zones increase (Table 8).

The average numbers of arcs and nodes within a partitioned network (i.e., a zone) decrease as the number of zones increases. In other words, the size of a zone is influenced by the number of zones in the original supply chain network. This reduces the optimization time because it directly increases speed of each simulation run. To be more specific, in ABS, a list of suppliers (i.e., farms and storage facilities) for each refinery is narrowed down so that a refinery does not need to check available suppliers in other zones. With 24 biorefineries looking for supplier every day, 0.1 milliseconds search time reduction saves 0.876 s (= 0.0001 s × 24 biorefineries × 365 days) from each simulation run. This will eventually reduce 0.146 hours in the simulation-based optimization with 600 simulation runs (= 20 iterations × 30 replications). Thus, we can conclude that the proposed partitioning algorithm lessens not only the number of transportation quantity variables (see Section 3.4) but also simulation run-time.

However, the computational efficiency does not guarantee that we can find the (near) optimal solution. Regarding the total cost of each case, the best solution can be achieved with the non-partitioning case (i.e., a network with one zone). Nevertheless, the case with two zones gives us the (near) optimal solution similarly to that of the non-partitioning case. The p-value of the paired t-test

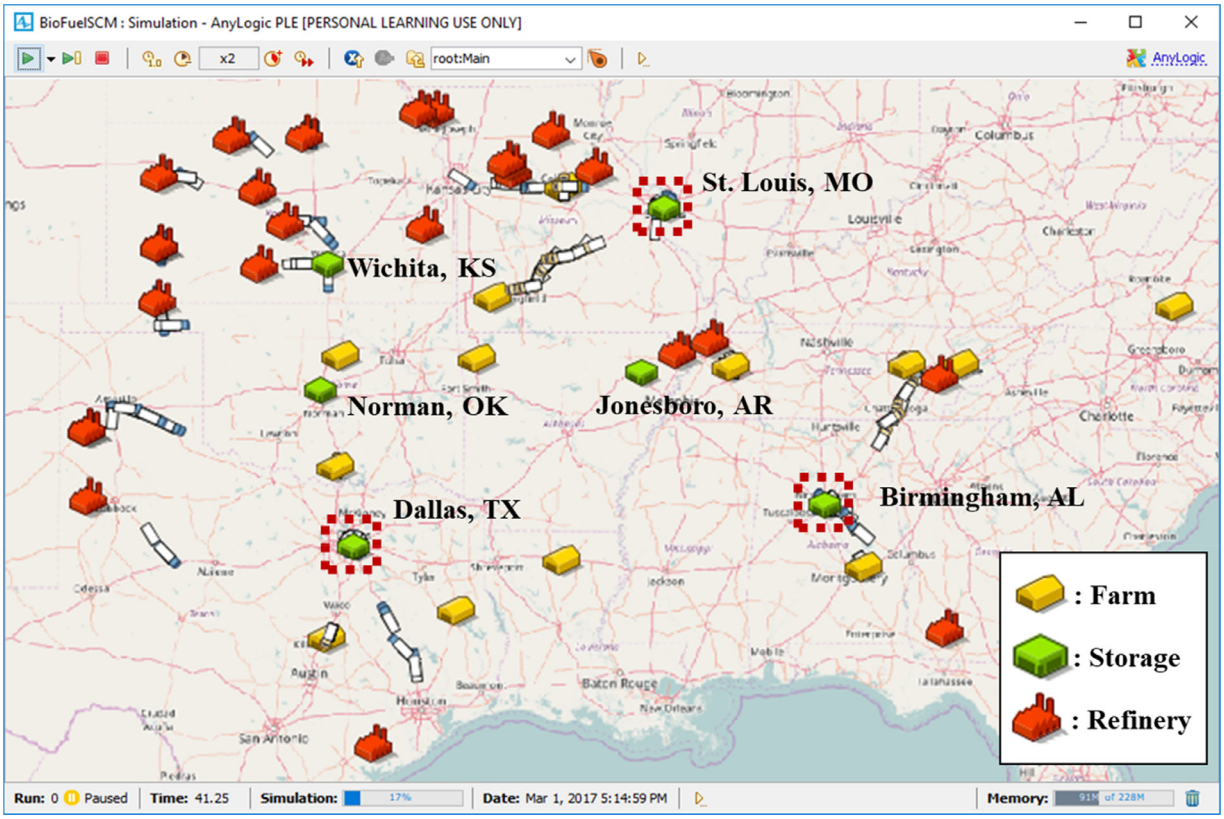

Fig. 7. Snapshot of AnyLogic simulation (dotted square: selected candidate storage sites).

Table 8
Performance of partitioned networks.

Category	Number of zones				
	1[a]	2	3	4	5
Number of arcs (arcs/zone)	534	143.5	59.3	33.5	21.2
Number of nodes (arcs/zone)	43	22.5	15.3	11.8	9.6
Length of arcs (miles/arc)	638.5	428.1	319.4	232.6	156.2
Travel distance (miles/truck)	625.0	640.8	653.4	652.3	696.8
Travel time (hours/truck)	10.4	10.7	10.9	10.8	11.6
Number of shipments(trucks/day)	188	188	188	188	188
Optimization time (hours)	1.7	1.5	1.4	1.2	1.1
Number of iterations	20	20	20	20	20
Total cost ($1,000/day)	107.2	108.1	110.5	110.9	116.1
Transportation cost ($1,000/day)	85.4	87.7	89.3	89.4	95.2
Holding cost ($1,000/day)	21.8	20.4	21.2	21.5	20.9

[a] Refers the original biomass supply chain network.

between two solutions at $\alpha = 0.05$ is 0.3472, so that there is no significant difference between the two solutions. *P*-values of other three cases are 0.1926 (3 zones), 0.1834 (4 zones), and 0.00348 (5 zones). Thus, in the subject network, the optimization with four zones still provides us the solution statistically similar to that of the non-partitioning case. Regarding that, the network partitioning can quickly find the (near)optimal solution without sacrificing accuracy of the original solution. It is better to use the partitioning algorithm, particularly when we are dealing with a large-scale supply chain network.

5. Conclusions and future research

This study has introduced the two-phase simulation-based location-allocation approach of biofuel storage facilities to minimize transportation cost of a biomass supply chain. The approach includes two major functions: (1) knowledge-based plant yield estimation with ALMANAC and (2) transportation cost estimation with ABS involving GIS. Since the ALMANAC model considers

environmental dynamics such as water use, soil nutrition, and plant competition for its estimation, it provides highly accurate estimation about potential yields of energy plants (i.e., switchgrass) across multiple locations in Southern Great Plains of U.S. Based on the estimated plant yields, the ABS with GIS has computed transportation costs regarding detail activities (e.g., loading, unloading, and storing feedstocks) among the actors (e.g. farms, storage facilities, and biorefineries) in the supply chain. The locations of storage facilities are found via the OptQuest® meta-heuristic optimization engine available in AnyLogic. In the experiments, performance of the proposed approach in terms of solution accuracy and computational efficiency has been discussed under two conditions: (1) different numbers for the partitioned network and (2) different numbers of biofuel storage facilities. The results have shown that the proposed simulation-based optimization approach can be used in practice because it significantly reduces computational demand of the original optimization approach. Moreover, it considers details of plant growth and supply chain activities so that a user can achieve realistic locations of biofuel storage facilities.

In future, the proposed approach will be expanded with detail activities (e.g., plant processing to generate ethanol at a refinery and warehousing operation at a biofuel storage) of each actor in a biomass supply chain to enhance its modeling accuracy. The integration of other activities into the proposed approach will provide us additional opportunities to find better locations of biofuel storage facilities. In addition, further validation efforts with real performance data given by biofuel supply chains using switchgrass are needed to address usability of the proposed approach.

References

[1] A.J. Ashworth, S.A. Weiss, P.D. Keyser, F.L. Allen, D.D. Tyler, A. Taylor, K.P. Beamer, C.P. West, D.H. Pote, Switchgrass composition and yield response to alternative soil amendments under intensified heat and drought conditions, Agric. Ecosyst. Environ. 233 (2016) 415–424.
[2] I. Awudu, J. Zhang, Uncertainties and sustainability concepts in biofuel supply chain management: a review, Renewable Sustain. Energy Rev. 16 (2) (2012) 1359–1368.
[3] J. Ben-Iwo, V. Manovic, P. Longhurst, Biomass resources and biofuels potential for the production of transportation fuels in Nigeria, Renewable Sustain. Energy Rev. 63 (2016) 172–192.
[4] B.M.M. Bomani, D.L. Bulzan, D.I. Centeno-Gomez, R.C. Hendricks, Biofuels As an Alternative Energy Source for Aviation-A Survey, NASA Glenn Research Center, Cleveland, Ohio, 2009.
[5] D. Bransby, P. Huang, Twenty-year biomass yields of eight switchgrass cultivars in Alabama, BioEnergy Res. 7 (4) (2014) 1186–1190.
[6] C.W. Chen, Y. Fan, Bioethanol supply chain system planning under supply and demand uncertainties, Transp. Res. Part E 48 (1) (2012) 150–164.
[7] Y.L. Chiew, T. Iwata, S. Shimada, System analysis for effective use of palm oil waste as energy resources, Biomass Bioenergy 35 (7) (2011) 2925–2935.
[8] F. Cherubini, The biorefinery concept: using biomass instead of oil for producing energy and chemicals, Energy Convers Manage. 51 (7) (2010) 1412–1421.
[9] S. de Jong, R. Hoefnagels, E. Wetterlund, K. Pettersson, A. Faaij, M. Junginger, Cost optimization of biofuel production—the impact of scale, integration, transport and supply chain configurations, Appl. Energy 195 (2017) 1055–1070.
[10] J.P. de Koff, D.D. Tyler, Improving switchgrass yields for bioenergy production, Carter (2012) 2011.
[11] B.E. Duran, D.S. Duncan, L.G. Oates, C.J. Kucharik, R.D. Jackson, Nitrogen fertilization effects on productivity and nitrogen loss in three grass-based perennial bioenergy cropping systems, PloS One 11 (3) (2016) e0151919.
[12] J. Dumortier, Impact of agronomic uncertainty in biomass production and endogenous commodity prices on cellulosic biofuel feedstock composition, GCB Bioenergy 8 (2016) 35–50, http://dx.doi.org/10.1111/gcbb.12238.
[13] EIA, Monthly Energy Rev. U.S. Energy Information Administration (2017).
[14] S.D. Ekşioğlu, A. Acharya, L.E. Leightley, S. Arora, Analyzing the design and management of biomass-to-biorefinery supply chain, Comput. Ind. Eng. 57 (4) (2009) 1342–1352.
[15] P.L. Eranki, B.D. Bals, B.E. Dale, Advanced regional biomass processing depots: a key to the logistical challenges to the cellulosic biofuel industry, Biofuels Bioprod. Bioref. 5 (2011) 621–630.
[16] J.H. Fike, J.W. Pease, V.N. Owens, R.L. Farris, J.L. Hansen, E.A. Heaton, E.A. Hong, H.S. Mayton, R.B. Mitchell, D.R. Viands, Switchgrass nitrogen response and estimated production costs on diverse sites, GCB Bioenergy (2017).
[17] M. Haque, F.M. Epplin, Switchgrass to ethanol: a field to fuel approach, Selected Paper presented at the Annual Meeting of the Agricultural and Applied Economics Association, Denver, CO, 2010, July.
[18] J.R. Hess, C.T. Wright, K.L. Kenney, Cellulosic biomass feedstocks and logistics for ethanol production, Biofuels Bioprod. Bioref. 1 (2007) 181–190.
[19] Y. Huang, C.W. Chen, Y. Fan, Multistage optimization of the supply chains of biofuels, Transp. Res. Part E 46 (6) (2010) 820–830.
[20] Jimmy Carter Plant Materials Center, Plant fact sheet for switchgrass (Panicum virgatum L.), USDA-Natural Resources Conservation Service (2011).
[21] T.P. Kandel, Y. Wu, V.G. Kakani, Growth and yield responses of switchgrass ecotypes to temperature, Am. J. Plant Sci. 4 (06) (2013) 1173.
[22] M.K. Kering, J.T. Biermacher, T.J. Butler, J. Mosali, J.A. Guretzky, Biomass yield and nutrient responses of switchgrass to phosphorus application, BioEnergy Res. 5 (1) (2012) 71–78.
[23] S. Kim, A. Williams, J.R. Kiniry, C.V. Hawkes, Simulating diverse native C 4 perennial grasses with varying rainfall, J.Arid Environ. 134 (2016) 97–103.
[24] S. Kim, J.R. Kiniry, A.S. Williams, N. Meki, L. Gaston, M. Brakie, A. Shadow, F.B. Fritschi, Y. Wu, Adaptation of C4 bioenergy crop species to various environments within the Southern Great Plains of USA, Sustainability 9 (1) (2017) 89.
[25] S. Kim, Y.J. Son, Y. Tian, Y.C. Chiu, C.D. Yang, Cognition-based hierarchical en route planning for multi-agent traffic simulation, Expert Syst. Appl. 85 (2017) 335–347.
[26] J.R. Kiniry, J.R. Williams, P.W. Gassman, P. Debaeke, A general, process-oriented model for two competing plant species, Trans. ASAE 35 (3) (1992) 801–810.
[27] J.R. Kiniry, M.A. Sanderson, J.R. Williams, C.R. Tischler, M.A. Hussey, W.R. Ocumpaugh, R.L. Reed, Simulating Alamo switchgrass with the ALMANAC model, Agron. J. 88 (4) (1996) 602–606.
[28] J.R. Kiniry, K.A. Cassida, M.A. Hussey, J.P. Muir, W.R. Ocumpaugh, J.C. Read, J.R. Williams, Switchgrass simulation by the ALMANAC model at diverse sites in the southern US, Biomass Bioenergy 29 (6) (2005) 419–425.
[29] J.R. Kiniry, M.R. Schmer, K.P. Vogel, R.B. Mitchell, Switchgrass biomass simulation at diverse sites in the northern Great Plains of the US, BioEnergy Res. 1 (3-4) (2008) 259–264.
[30] J.R. Kiniry, M.V.V. Johnson, S.B. Bruckerhoff, J.U. Kaiser, R.L. Cordsiemon, R.D. Harmel, Clash of the titans: comparing productivity via radiation use efficiency for two grass giants of the biofuel field, BioEnergy Res. 5 (1) (2012) 41–48.
[31] J.R. Kiniry, L.C. Anderson, M.V. Johnson, K.D. Behrman, M. Brakie, D. Burner, C. Hawkes, Perennial biomass grasses and the mason—dixon line: comparative productivity across latitudes in the southern great plains, BioEnergy Res. 6 (1) (2013) 276–291.
[32] E.L. Lawler, D.E. Wood, Branch-and-bound methods: A survey, Operations Res. 14 (4) (1966) 699–719.
[33] I. Lewandowski, J.M. Scurlock, E. Lindvall, M. Christou, The development and current status of perennial rhizomatous grasses as energy crops in the US and Europe, Biomass Bioenergy 25 (4) (2003) 335–361.
[34] M.K. Lim, Y. Ouyang, Biofuel Supply Chain Network Design and Operations, Environmentally Responsible Supply Chains, Springer International Publishing, 2016, pp. 143–162.
[35] A.W. Magazine, F. Economy, Ethanol production, along with other factors, affects agricultural commodity markets, USDA-Economic Research Service. Retrieved

from, 2017, Mar. 23. https://www.ers.usda.gov/topics/farm-economy/bioenergy/findings/, .
[36] S.B. McLaughlin, L.A. Kszos, Development of switchgrass (Panicum virgatum) as a bioenergy feedstock in the United States, Biomass Bioenergy 28 (6) (2005) 515–535.
[37] U. NASS, Usual Planting and Harvesting Dates for US Field Crops. Agricultural Handbook 628 (1997).
[38] National Agricultural Statistics Service, Crop production: 2015 Summary, United States Department of Agriculture (USDA), 2016 ISSN.
[39] National Oceanic and Atmospheric Administration (NOAA) station, Sep. 7, Climate Data Online Search (2017) Retrieved from http://www.ncdc.noaa.gov/cdo-web/search.
[40] Natural Resources Conservation Service, Sep. 7, Web Soil Survey (2017) Retrieved from http://websoilsurvey.sc.egov.usda.gov/App/WebSoilSurvey.aspx.
[41] L.D. Quinn, K.C. Straker, J. Guo, S. Kim, S. Thapa, G. Kling, D.K. Lee, T.B. Voigt, Stress-tolerant feedstocks for sustainable bioenergy production on marginal land, BioEnergy Res. 8 (3) (2015) 1081–1100.
[42] REN21, *Renewable Energy Policy Network for the 21st Century 2015. Renewables 2015 Global Status Report.* REN21, Rue de Milan, France.
[43] RFA, Ethanol Industry Outlook, Renewable Fuels Association, 2016.
[44] M.R. Schmer, K.P. Vogel, R.B. Mitchell, R.K. Perrin, Net energy of cellulosic ethanol from switchgrass, Proc. Natl. Acad. Sci. 105 (2) (2008) 464–469.
[45] M.G. Tulbure, M.C. Wimberly, V.N. Owens, Response of switchgrass yield to future climate change, Environ. Res. Lett. 7 (4) (2012) 045903.
[46] W.J. Stevenson, Operations Management, 12th Edition, McGraw-Hill/Irwin, New York, NY, 2014.
[47] E.K. Vakkilainen, Steam Generation from Biomass, 1st Edition, Butterworth-Heinemann, Cambridge, MA, 2016.
[48] D.A.N. Wang, D.S. Lebauer, M.C. Dietze, A quantitative review comparing the yield of switchgrass in monocultures and mixtures in relation to climate and management factors, GCB Bioenergy 2 (1) (2010) 16–25.
[49] K. Warwick, F.L. Allen, P.D. Keyser, A.J. Ashworth, G.E. Bates, D.D. Tyler, C.A. Harper, Biomass and integrated forage/biomass yields of switchgrass as affected by intercropped cool-and warm-season legumes, J. Soil Water Conserv. 71 (1) (2016) 21–28.
[50] M.J. Williams, J. Douglas, Planting and Managing Giant Miscanthus as a Biomass Energy Crop 30 USDA-NRCS Plant Materials Program, Washington, DC Technical Note,(4), 2011.
[51] L. Wright, A. Turhollow, Switchgrass selection as a “model” bioenergy crop: a history of the process, Biomass Bioenergy 34 (6) (2010) 851–868.
[52] D. Yue, F. You, S.W. Snyder, Biomass-to-bioenergy and biofuel supply chain optimization: overview, key issues and challenges, Comput. Chem. Eng. 66 (2014) 36–56.
[53] F. Zhang, D. Johnson, M. Johnson, D. Watkins, R. Froese, J. Wang, Decision support system integrating GIS with simulation and optimisation for a biofuel supply chain, Renewable Energy 85 (2016) 740–748.
[54] S. Lloyd, Least squares quantization in PCM, IEEE transactions on information theory 28 (2) (1982) 129–137.
[55] A.A. Rentizelas, I.P. Tatsiopoulos, A. Tolis, An optimization model for multi-biomass tri-generation energy supply, Biomass and bioenergy 33 (2) (2009) 223–233.